Wide-range-adjusted threshold voltages for E-mode AlGaN/GaN HEMT with a p-SnO cap gate

Dazheng Chen[1†*], Peng Yuan[1†], Shenglei Zhao[1], Shuang Liu[1], Qian Xin[2], Xiufeng Song[1], Shiqi Yan[2], Yachao Zhang[1], He Xi[1], Weidong Zhu[1], Weihang Zhang[1], Jiaqi Zhang[1], Hong Zhou[1], Chunfu Zhang[1], Jincheng Zhang[1*] and Yue Hao[1]

ABSTRACT p-GaN cap layer has been recognized as a commercial technology to manufacture enhanced-mode (E-mode) AlGaN/GaN high electron mobility transistor (HEMT); however, the difficult activation of Mg doping and etching damage of p-GaN limit the further improvement of device performance. Thus, the more cost-effective cap layer has attracted wide attention in GaN-based HEMT. In this paper, p-type tin monoxide (p-SnO) was firstly investigated as a gate cap to realize E-mode AlGaN/GaN HEMT by both Silvaco simulation and experiment. Simulation results show that by simply adjusting the thickness (50 to 200 nm) or the doping concentration (3×10^{17} to $3 \times 10^{18} \, \text{cm}^{-3}$) of p-SnO, the threshold voltage (V_{th}) of HEMT can be continuously adjusted in the range from zero to 10 V. Simultaneously, the device demonstrated a drain current density above 120 mA mm^{-1}, a gate breakdown voltage (V_{BG}) of 7.5 V and a device breakdown voltage (V_{B}) of 2470 V. What is more, the etching-free AlGaN/GaN HEMT with sputtered p-SnO gate cap were fabricated, and achieved a positive V_{th} of 1 V, V_{BG} of 4.2 V and V_{B} of 420 V, which confirms the application potential of the p-SnO film as a gate cap layer for E-mode GaN-based HEMT. This work is instructive to the design and manufacture of p-oxide gate cap E-mode AlGaN/GaN HEMT with low cost.

Keywords: p-SnO gate cap, E-mode AlGaN/GaN HEMT, positive threshold voltage, wide-range adjustment, silvaco ATLAS, sputtered p-SnO

INTRODUCTION

Owing to the great advantages of large bandgap width, high breakdown field intensity, high polarization coefficient, high electron mobility, and saturated electron drift velocity [1,2], gallium nitride (GaN) heterostructures have been used in high electron mobility transistors (HEMTs) and found wide applications in power electronics. But the difficulty to realize enhanced-mode (E-mode) operation has become one of the key factors which limit their large-scale commercialization [3]. At present, the main solutions include recess gate structure [4], fluoride plasma treatment [5], p-type GaN (p-GaN) gate [6–10], and Cascode structure [11]. Among them, only the p-GaN gate

has been proved as a promising strategy in practical application. However, the threshold voltage (V_{th}) in p-GaN gate devices is relatively low (around 1 V) [12], which is due to that the Mg-doping in GaN is difficult to be activated and thus the low hole concentration may limit the further increase of V_{th}. Also the dry etching-induced damage would deteriorate the electrical characteristics and reliability of AlGaN/GaN HEMT [13].

In recent years, p-type metal-oxides (NiO, Cu$_2$O, etc.) have been used to fabricate E-mode AlGaN/GaN HEMT due to their high hole concentration and compatibility to wet etch process. Nevertheless, the V_{th} of HEMT with p-NiO and p-Cu$_2$O gate cap was generally around zero volt [14–18]. As we know, the principle of p-GaN cap to achieve E-mode operation lies in that, at zero bias voltage, the bottom of conduction band (E_c) can be raised above the Fermi level (E_f) of GaN to exhaust the two-dimensional electron gas (2DEG) under the gate. Unlike the conventional HEMT devices, the V_{th} of p-gate cap devices is related to the depth of the valence-band-top (E_v) rather than the E_c [19]. Due to the relatively low E_v levels of NiO or Cu$_2$O (~5.4 eV), the limited uplift ability of energy level at the AlGaN/GaN interface becomes an obstacle to obtain positive V_{th} in p-gate cap HEMTs. Therefore, a p-type oxide with sufficient E_v depth may be favorable for achieving E-mode GaN-based HEMT, but the further systematic investigation is lacking.

In this study, the AlGaN/GaN HEMTs with p-SnO ($E_v \approx$ 7.6 eV) and other oxide ($E_v > 5.4$ eV) gate caps have been systematically investigated by using the ATLAS in Silvaco TCAD and reported experimental parameters. As p-SnO film possesses large electron affinity, wide bandgap [20], high p-doping concentration ($5 \times 10^{18} \, \text{cm}^{-3}$), various deposition methods (sputter, e-beam, pulsed laser deposition, etc.) [21–24], and low treatment temperature, it has been successfully applied to p-channel thin film transistors (TFTs), p-n junctions, complementary metal oxide semiconductor (CMOS) logic circuits, and transparent devices [21,25,26]. Here, the simulation results showed that the V_{th} of AlGaN/GaN HEMT can be wide-range-controlled from zero to 10 V by simply adjusting the thickness (50 to 200 nm) or the doping concentration (3×10^{17} to $3 \times 10^{18} \, \text{cm}^{-3}$) of p-SnO. The device also demonstrated a drain current density above 120 mA mm^{-1}, a gate breakdown voltage (V_{BG}) of 7.5 V and a device breakdown voltage (V_{B}) over 2 kV. Further, the feasibility

[1] State Key Discipline Laboratory of Wide Bandgap Semiconductor Technology, School of Microelectronics, Xidian University, Xi'an 710071, China
[2] State Key Laboratory of Crystal Materials, Center of Nanoelectronics and School of Microelectronics, Shandong University, Jinan 250100, China
† These authors contributed equally to this work.
* Corresponding authors (emails: dzchen@xidian.edu.cn (Chen D); jchzhang@xidian.edu.cn (Zhang J))

of p-SnO gate cap has been experimentally verified. This work is instructive to the manufacture of cost-effective E-mode HEMT and the development of GaN-based power electronics.

METHOD

In order to ensure the reliability and accuracy, the model has been calibrated according to the report of gate injection transistor by Uemoto *et al.* in 2007 [27]. As shown in Fig. 1a, when the gate voltage (V_G) is 6 V, the drain current density reaches 260 mA mm^{-1} in the transfer curve, and the V_{th} is 1 V. In the output curves (inset in Fig. 1a), the drain saturation current density reaches 200 mA mm^{-1} when the V_G is set as 5 V. Both of them agree well with the reference. After model calibrating, the basic characteristics of AlGaN/GaN HEMT (Fig. 1b) with p-SnO and other oxide (such as Cu$_2$O, NiO, WO$_3$, MoO$_3$, and V$_2$O$_5$) gate caps have been simulated by ATLAS in Silvaco TCAD. In details, the structure of p-SnO gate cap HEMT consists of a substrate (Si, SiC, or sapphire), 3 μm GaN semi-insulating layer, 200 nm GaN channel layer, 20 nm Al$_{0.2}$Ga$_{0.8}$N barrier layer, 150 nm p-SnO layer, and Si$_3$N$_4$ passivation layer. The gate-source length (L_{GS}), gate length (L_G), gate width (W_G), and gate-drain length (L_{GD}) are 2.5, 5, 50, and 11.5 μm, respectively. Here the influence of the thickness, doping concentration, bandgap of p-SnO on the V_{th}, and the underlying mechanism have been studied. The detail calculation method can be found in our previous work [28], and all the parameters including bandgap, dielectric constants, electron affinity, E_v and E_c for oxides come from the experimental reports [14,29–32].

RESULTS AND DISCUSSION

Basic characteristics of p-SnO gate cap HEMT

The V_{th} of AlGaN/GaN HEMT is generally defined as the gate bias voltage when the drain current density reaches 1 mA mm^{-1} under 10 V drain voltage (V_D). As shown in Fig. 2a, the p-SnO gate cap HEMT has obtained a positive V_{th} of 3.2 V, which reveals the E-mode operation of HEMT and the value of V_{th} could meet the requirements of power applications. Especially, a doping concentration as high as 2×19 cm^{-3} of p-GaN is necessary to realize E-mode HEMT [33], while here a much lower doping concentration of 7×17 cm^{-3} for p-SnO is enough and this p-SnO film could be easily achieved by several deposition methods at a lower cost. From Fig. 2b, the saturation drain current density of the device can reach 120 mA mm^{-1}

when $V_G = 8$ V, and the specific on-resistance (R_{ON}) [34] is about 3.8 mΩ cm^2. In Fig. 2c, under a V_G of zero and drain current density of 1 mA mm^{-1}, the V_B can reach 2470 V. Therefore, besides the more positive V_{th}, the basic performance of p-SnO gate cap HEMT can also satisfy the needs of practical applications.

Meanwhile, the gate leakage current and breakdown characteristics of AlGaN/GaN HEMTs with the p-SnO or p-GaN gate caps have been simulated. It is clear the gate leakage current density in p-SnO gate cap HEMT is much lower than that in p-GaN device (inset in Fig. 2d). This can be explained by the behaviors of the schottky diode (gate-metal/p-cap) and PIN diode (p-cap/AlGaN/GaN). The schottky diode is reverse-cut off when a positive V_G is applied, and the PIN diode will be turned off at a negative V_G and the depletion region will expand, both of which could act as a blocker of gate leakage current [35]. Due to the deeper E_v of p-SnO than p-GaN, the relatively high schottky barrier is thus responsible for the lower gate leakage current in corresponding devices. On the other hand, the gate breakdown voltage is another key parameter to HEMT. Under a V_D of zero and gate current density of 1 mA mm^{-1}, the extracted gate breakdown voltage of p-SnO device (7.5 V) is also higher than that of the p-GaN device (6 V), as shown in Fig. 2d.

V_{th} regulation of p-SnO gate cap HEMT

For p-SnO HEMT in Fig. 3a, with the increase of SnO thickness from 50 to 200 nm or the doping concentration of SnO from 3×10^{17} to 3×10^{18} cm^{-3}, the V_{th} of AlGaN/GaN HEMT can be controlled in a large range from 0 to 10 V. Typically, it can be seen from Fig. 3b that the V_{th} are 0, 1.2, 2.4, 3.6, 4.8, 6.1, and 7.3 V when the doping concentration of p-SnO locates between 4×10^{17} and 1×10^{18} cm^{-3}. Similarly, the increased V_{th} (0.5, 1.5, 2.8, 4.5, 6.4, and 8.6 V) can be obtained in Fig. 3c when the thickness of p-SnO changes from 100 to 200 nm. As a result, the V_{th} can be wide-range-controlled by simply adjusting the thickness or doping concentration of p-SnO, which is favorable to the fabrication of power devices.

To understand the physical mechanism, Fig. 3d shows the energy band diagrams in the gate region of p-SnO HEMT at the SnO doping concentrations of 6×10^{17}, 8×10^{17}, 1×10^{18} and 2×10^{18} cm^{-3}. For the PIN diode (p-SnO/AlGaN/GaN), it is well known in the pn junction theory that the depletion width in p-SnO decreases with its doping concentration, while the depletion region in the GaN side will expand accordingly. This means that
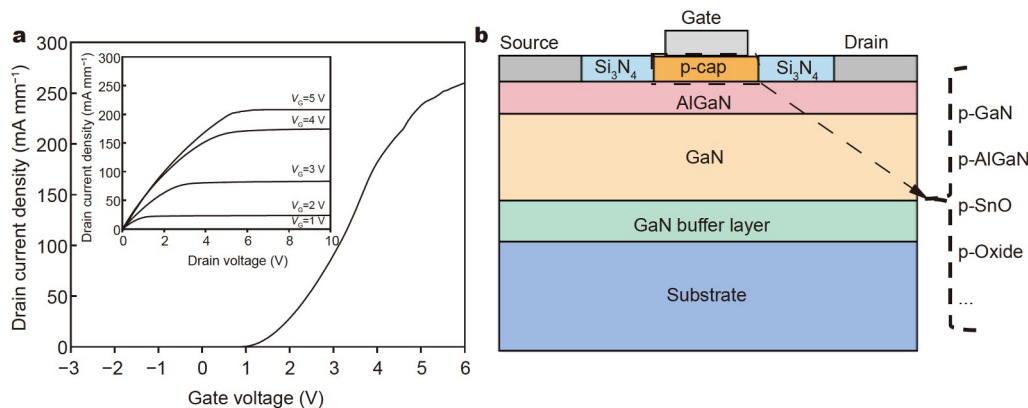
Figure 1 Simulated (a) transfer and output curves in model calibrating, and (b) device structure of p-cap AlGaN/GaN HEMT.
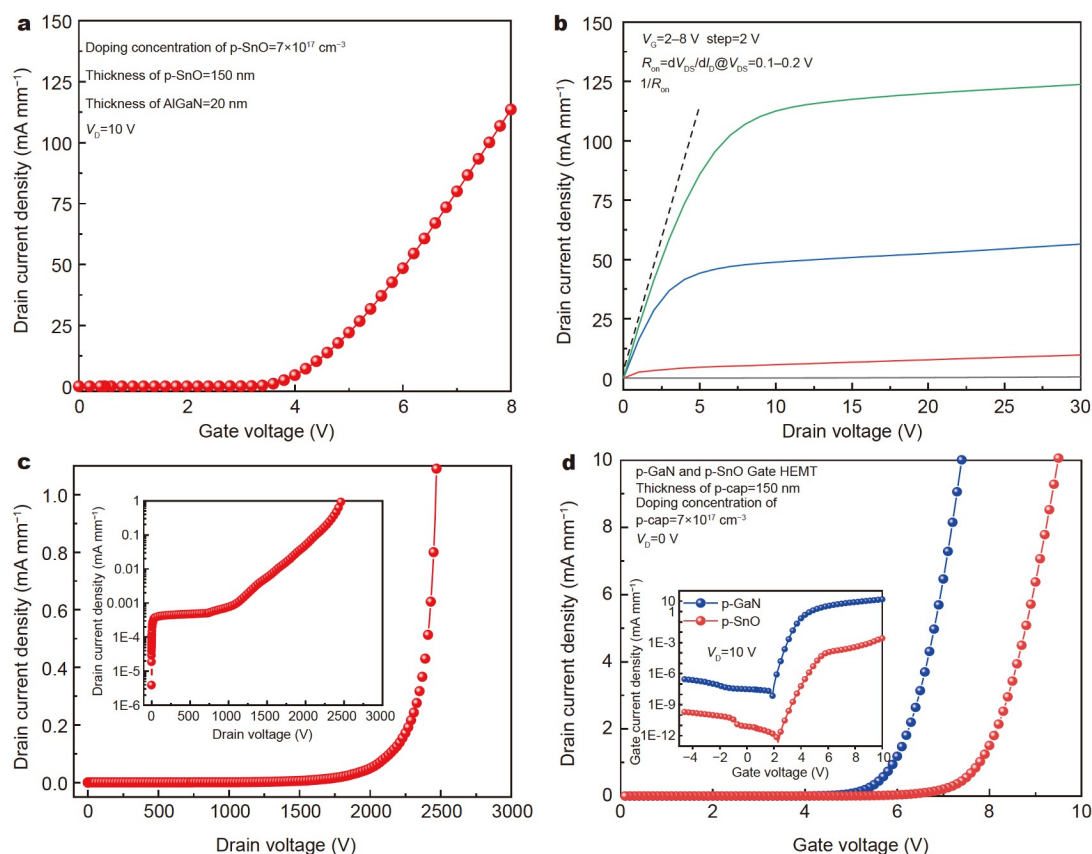
Figure 2 Simulated (a) transfer, (b) output, and (c) breakdown characteristics of the p-SnO gate cap HEMT; (d) gate leakage current density and gate breakdown characteristic of AlGaN/GaN HEMT with the p-SnO or p-GaN gate cap.

more electrons have been exhausted, in other words, the E_c of GaN at the AlGaN/GaN interface will be far away from E_f. Consequently, large V_G (V_{th}) must be applied to open the 2DEG channel. Simultaneously, when the doping concentration is specified and the thickness of SnO increases from 50 to 150 nm (as shown in Fig. 3e), the depletion of 2DEG under the gate will be intensified and the operation of 2DEG channel must consume larger V_G. In addition, in Fig. 3f, g, with the increase of doping concentration and thickness of p-SnO cap, the gradually expanded depletion zone under the gate would induce the decreased gate leakage current density and increased gate breakdown voltage. This tendency is consistent with the changes of V_{th}, in other words, it is possible to achieve a large V_{th} and high gate breakdown voltage at the same time.

**V_{th} stability of p-SnO gate cap HEMT**
As the SnO film can be deposited by various process and treatment methods [36–39], the bandgap fluctuation of p-SnO film was unavoidable, which may also affect the device performance. As shown in Fig. 4a, the V_{th} is nearly proportional to the bandgap, which coincides with the V_{th} expression proposed in the previous literature [19]. Even at a low bandgap of 2.7 eV, the V_{th} can also reach 2.3 V. This insensitivity of V_{th} to the bandgap fluctuation may enlarge the process window and enrich the deposition method selections for p-SnO gate cap, which is desired to the cost-effective power electronics in the future.

Furthermore, the interface state between p-SnO and (Al)GaN is another factor affecting the device performance. According to

the reports of (Al)GaN MOS-HEMT, the polarity, energy level positions, and concentrations of interface traps may cause the instability of V_{th} [40,41]. Therefore, we assumed two defect levels ($E_1 = E_c - 0.5$ eV, $E_2 = E_v + 0.5$ eV) and two defect densities (1×10^{13} and 1×10^{11} cm^{-2}) at the p-SnO/AlGaN interface. The two acceptor-like discrete states ($E_A(H)$, $E_A(L)$) with different defect densities were placed at E_2, and two donor-like discrete states ($E_D(H)$, $E_D(L)$) with different defect densities were placed at E_1. In order to simulate the influence of defects on V_{th}, the above four interface defects are introduced at 1 nm above and below the p-SnO/AlGaN interface. It is clear from Fig. 4b that V_{th} presents a negative drift (the donor state) or a positive drift (the acceptor state) behavior with respect to the ideal characteristics, and the higher the trap density, the greater the effect on V_{th}. It can be observed that the drift of V_{th} is 0.2 V when the density is 1×10^{11} cm^{-2}, which reaches 3.4 V (positive drift) and 2.3 V (negative drift) at a density of 1×10^{13} cm^{-2}. Therefore, during the device fabrication, the interface defects should be reduced as much as possible to ensure good device performance. Also, when an acceptor trap at E_1 or a donor trap at E_2 is assumed, no changes in V_{th} can be seen as the states are neutral in the voltage bias ranging from 0 to 10 V, which agrees with the previous report [42]. Besides these inner defects, the outer factors may also affect the V_{th} of device. For example, the water molecules adsorbed on the surface of the p-SnO film would produce additional charges by ionization and induce the changes of the V_{th} at a bias of V_G [43], thus the device passivation is essential to improve the V_{th} stability. In fact, the interface states are a very
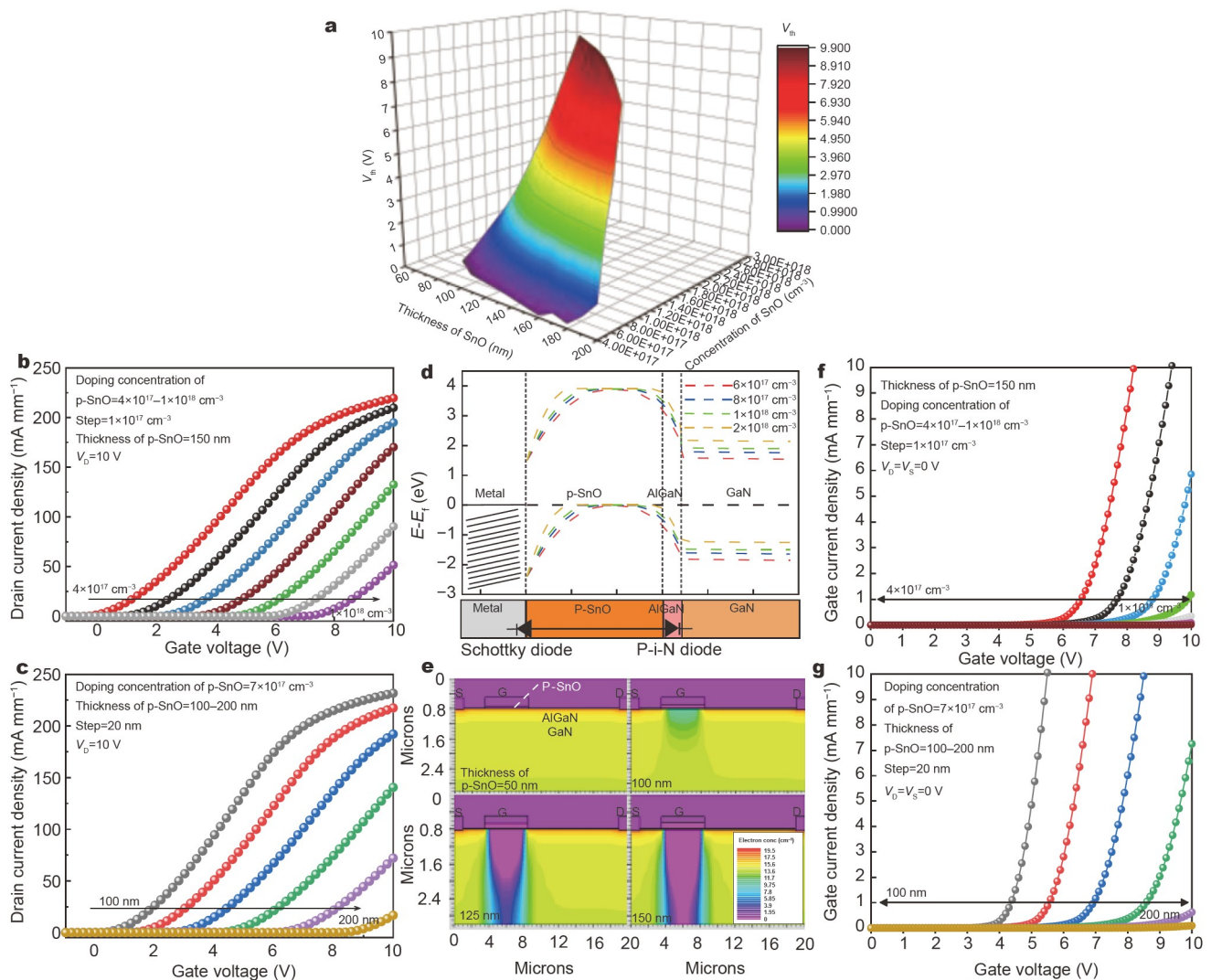
Figure 3 Dependence of simulated (a) V_{th}, (b, c) transfer characteristics, (d) energy band diagram, (e) electron concentration distributions, and (f) gate leakage current density on the p-SnO doping concentration and/or thickness for AlGaN/GaN HEMTs.
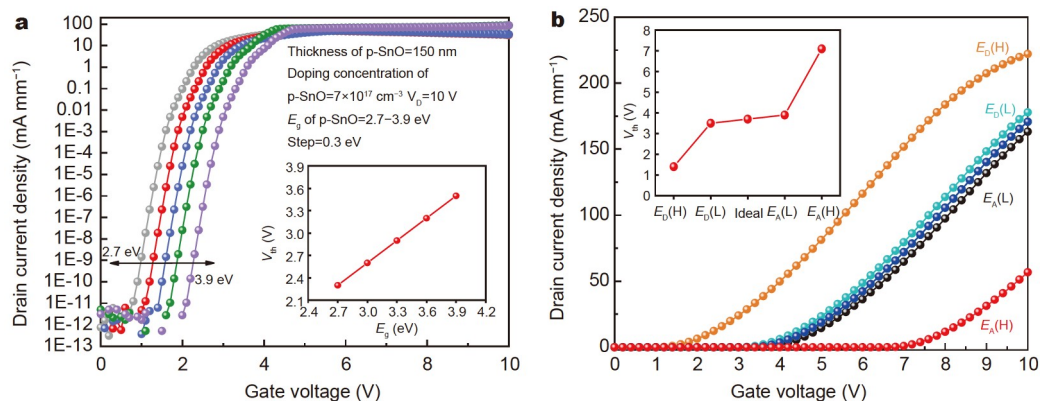
Figure 4 Simulated transfer characteristic curves of p-SnO gate cap HEMT (a) with various SnO bandgap values and (b) defects at SnO/AlGaN interface.

complex problem, and therefore more experimental studies should be carried out to understand the mechanism of V_{th} stability beyond the simulations, which will be investigated in our next work.

Experimental verification of p-SnO gate cap HEMT

The p-SnO gate cap HEMT consists of a substrate layer (sapphire), a GaN semi-insulating layer, a 200-nm GaN channel layer, a 20-nm $Al_{0.2}Ga_{0.8}N$ barrier layer, and a 40-nm p-SnO

layer. The L_{GS}, L_G, W_G and L_{GD} are 4, 2, 50 and 12 μm, respectively. Fig. S1 presented the key process steps of AlGaN/GaN epitaxial growth and device fabrication. Here, the ohmic metal deposition and annealing (850°C) were processed before the p-SnO gate cap, as the phase of SnO is metastable and temperature-sensitive, the high temperature would accelerate the phase separation of SnO into metallic β-Sn-rich phase [44]. At the same time, considering limited temperature resistance of photoresist, the 40-nm thick SnO layer was deposited by magnetron sputtering with 50 W radio-frequency power and 5.7 mTorr (1 mTorr = 0.133 Pa) growth pressure in $O_2/Ar+O_2$ (3.1%) mixed atmosphere, followed by the lift-off process, and then the samples were annealed at 225°C in air to obtain the patterned p-SnO cap layer. The X-ray diffraction (XRD, Fig. 5a and Fig. S2), optical bandgap (Fig. S3), and atomic force microscopy (AFM, Fig. 5b and Fig. S4) results of p-SnO film (on sapphire) from the same batch proved that the p-SnO cap layer has been well formed. After the evaporation of gate metal (Ni/Au), the AlGaN/GaN HEMTs with p-SnO gate cap were fabricated. Particularly, the room-temperature sputtering and low-temperature air annealing method for p-SnO, proposed in our previous work [45], is perfectly compatible to the fabrication of GaN-based HEMTs. In addition, the metal gate HEMT has also been fabricated except for the p-SnO cap deposition, and the corresponding electrical properties can be found in Fig. S5.

For p-SnO gate cap HEMT, the measured transfer and output characteristics, gate leakage current density, gate and device breakdown curves are displayed in Fig. 5c–f. From the transfer characteristic curve, the V_{th} of the p-SnO gate cap HEMT can reach 1 V and the E-mode operation has been realized. Compared with the metal gate HEMT, the V_{th} was shifted forward by about 3 V, which is superior to that of the experimentally reported HEMTs with the p-oxide (NiO, Cu_2O) gate caps [14,29]. Simultaneously, the p-SnO gate cap HEMT achieved a reverse gate leakage current density of 6×10^{-6} mA mm^{-1} and a drain current density of 18 mA mm^{-1} when the $V_G = 4$ V, as shown in Fig. 5c, d. Fig. 5e, f show that the gate was broken down near 4.2 V ($V_D = 0$ V) and the device breakdown voltage reached 420 V. According to the breakdown curves at $V_G = 0$ V (Fig. 5f), the off-state leakage current at gate (I_G) is responsible for the device breakdown. Although the experimental results well verify the feasibility of p-SnO as the gate cap of E-mode HEMT, the drain current density is still lower than that of the mainstream p-GaN gate HEMTs. This can be partly explained by the transconductance characteristic in the inset of Fig. 5c. Although the transconductance value rapidly increased with the gate voltage (from 0 to 4 V), the relatively low V_{BG} (4.2 V) limited the possible improvement of drain current density. This is due to the first adoption of p-SnO gate without optimization, and the quality of p-SnO film, SnO/(Al)GaN interface, and metal contact needs to be further optimized. Therefore, more careful device designs and process adjustments would be performed in our future work to explore and improve the performance of p-SnO gate cap HEMTs.
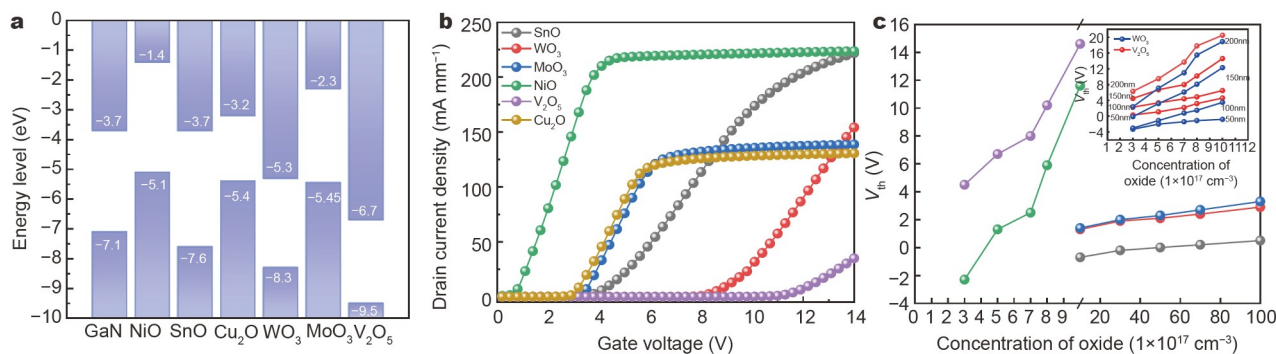
Other p-type oxide gate cap HEMTs

The typical p-type oxides, such as Cu_2O, NiO, WO_3, MoO_3 and V_2O_5, have been selected as the p-type gate caps in the AlGaN/GaN HEMTs to construct the E-mode devices.

Fig. 6a displays the energy band diagrams of various oxides and GaN. All the values are originated from the Refs. [14,29–32] and the structure parameters of devices are completely consistent. From the simulated transfer characteristic curves in Fig. 6b, the positive V_{th} has been observed in all HEMTs with various oxide gate caps. It should be mentioned that the doping concentrations of SnO, WO_3 and V_2O_5 are 8×10^{17} cm^{-3}, and the V_{th} of the corresponding devices are 4.0, 8.0 and 11 V, respectively. Although the doping concentrations of NiO, Cu_2O
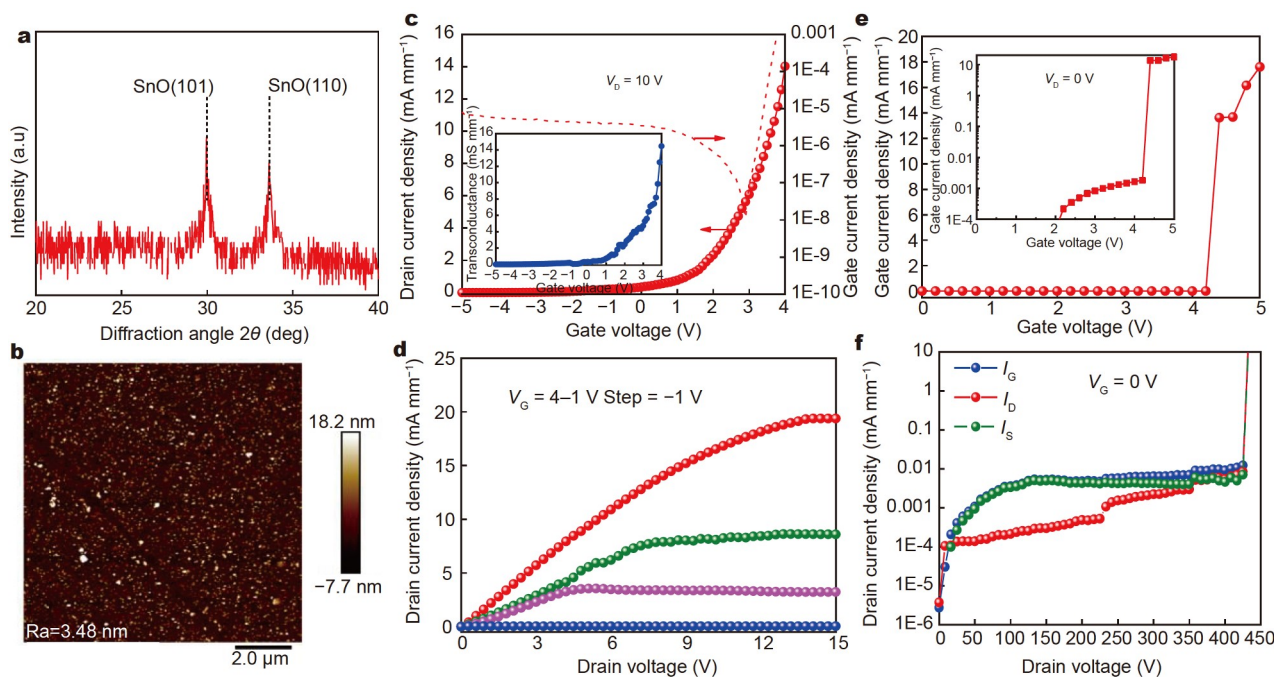
Figure 5 (a) X-ray diffraction pattern and (b) AFM image of p-SnO film on sapphire substrate; measured (c) transfer and transconductance characteristics, gate leakage current density, (d) output, (e) gate breakdown, and (f) device breakdown characteristics of p-SnO gate cap HEMT. Here the I_G, I_D and I_S represented the off-state leakage current at gate, drain, and source, respectively.

Figure 6 Simulated (a) energy band diagrams of p-type oxides and GaN, (b) transfer characteristic curves of p-type oxide gate cap HEMTs, and (c) threshold voltage regulation of p-type oxide gate cap devices with different doping concentrations and thicknesses of p-type oxides.

and MoO_3 are higher than 1×10^{19} cm^{-3}, the devices can only obtain a smaller V_{th}. It is suggested that the deeper E_v of these oxides (Fig. 6a) make the main contribution to the more positive V_{th}, which can be proved by the theoretical formula of V_{th} for p-cap gate HEMT [19,46]:

$$V_{th} = \frac{E_{gp} + \Delta E_{c1} - \Delta E_{c2}}{q} + \frac{\delta_b}{2C_b} + \frac{C_{th}(E_g - E_{a2})}{C_{bq}} - \frac{\delta_{p2} - \delta_{p1}}{C_b}. \quad (1)$$

According to the formula, the V_{th} is determined by two parts, one is the E_v-related part of $E_{c,GaN} - E_{v,p-cap}$, a value equals to $E_{gp} + \Delta E_{c1} - \Delta E_{c2}$, where E_{gp} is the bandgap of the p-cap layer, ΔE_{c1} is the E_c offset at the p-cap/AlGaN interface, ΔE_{c2} is the E_c offset at the AlGaN/GaN interface. Another part is decided by the properties of AlGaN/GaN heterostructure. In consequent, the deeper E_v of p-cap material is, the greater value of $E_{c,GaN} - E_{v,p-cap}$, and the greater V_{th} will be obtained. This is well consistent with the changes of V_{th} in HEMTs (Fig. 6b) with different p-oxide gate caps possessing various E_v levels.

Additionally, it can be observed from Fig. 6c that the V_{th} of HEMTs with p-type WO_3 and V_2O_5 gate caps could be easily wide-range-adjusted by controlling the doping concentration, while the V_{th} values of devices with p-type NiO, Cu_2O, and MoO_3 gate caps are much smaller even at a high doping concentration of 1×10^{19} cm^{-3}. Besides the doping levels, the thickness of WO_3 and V_2O_5 gate caps can also be used to adjust the V_{th} (inset in Fig. 6c), and the relatively high V_{th} of V_2O_5 gate cap device can be attributed to its deeper E_v and stronger band uplift ability at the AlGaN/GaN interface. All of these confirm that the E_v depth of wide-bandgap p-oxides plays the crucial role in depleting the 2DEG at the AlGaN/GaN interface, and the E-mode AlGaN/GaN HEMTs are achievable by carefully controlling the doping concentration and thickness of p-oxide gate caps.

CONCLUSION

The V_{th} of AlGaN/GaN HEMT with p-SnO gate cap can be wide-range-controlled from zero to positive 10 V by simply adjusting the thickness or the doping concentration of p-SnO layer. In simulations, the device demonstrates a drain current density above 120 mA mm^{-1}, a V_{BG} of 7.5 V, and V_B over 2 kV. It has been suggested that the p-oxides with wide bandgap and deep E_v are promising gate cap selections for E-mode devices. Furthermore, the experimental AlGaN/GaN HEMT with the sputtered p-SnO gate cap achieved a positive V_{th} of 1 V, V_{BG} of 4.2 V and V_B of 420 V, which further verify the feasibility of p-

SnO as the gate cap of E-mode HEMT. This work is instructive to the design and manufacture of cost-effective GaN power electronic devices.

1 Kanamura M, Kikkawa T, Iwai T, et al. An over 100 W n-GaN/n-AlGaN/GaN MIS-HEMT power amplifier for wireless base station applications. In: IEEE International Electron Devices Meeting, 2005. IEDM Technical Digest. Washington, 2005. 572–575

2 Liu J, Zhou Y, Chu R, et al. Highly linear $Al_{0.3}Ga_{0.7}$N-$Al_{0.05}$/$Ga_{0.95}$/N-GaN composite-channel HEMTs. IEEE Electron Device Lett, 2005, 26: 145–147

3 Wurfl J, Hilt O, Bahat-Treidel E, et al. Technological approaches towards high voltage, fast switching GaN power transistors. ECS Trans, 2013, 52: 979–989

4 Oka T, Nozawa T. AlGaN/GaN recessed MIS-Gate HFET with high-threshold-voltage normally-off operation for power electronics applications. IEEE Electron Device Lett, 2008, 29: 668–670

5 Cai Y, Zhou Y, Lau KM, et al. Control of threshold voltage of AlGaN/GaN HEMTs by fluoride-based plasma treatment: From depletion mode to enhancement mode. IEEE Trans Electron Devices, 2006, 53: 2207–2215

6 Hu X, Simin G, Yang J, et al. Enhancement mode AlGaN/GaN HFET with selectively grown pn junction gate. Electron Lett, 2000, 36: 753–754

7 Tsuyukuchi N, Nagamatsu K, Hirose Y, et al. Low-leakage-current enhancement-mode AlGaN/GaN heterostructure field-effect transistor using p-type gate contact. Jpn J Appl Phys, 2006, 45: 319–321

8 Sugiyama T, Amano H, Iida D, et al. High-temperature operation of normally off-mode AlGaN/GaN heterostructure field-effect transistors with p-GaN gate. Jpn J Appl Phys, 2011, 50: 01AD03

9 Hwang I, Choi H, Lee JW, et al. 1.6 kV, 2.9 mΩ cm^2 normally-off p-GaN HEMT device. In: 2012 24th International Symposium on Power Semiconductor Devices and ICs. Bruges, 2012. 41–44

10 Hwang I, Kim J, Choi HS, et al. p-GaN gate HEMTs with tungsten gate metal for high threshold voltage and low gate current. IEEE Electron Device Lett, 2013, 34: 202–204

11 Zhang J, Zhang W, Wu Y, et al. Wafer-scale Si-GaN monolithic integrated E-mode cascode FET realized by transfer printing and self-aligned etching technology. IEEE Trans Electron Devices, 2020, 67: 3304–3308

12 Erofeev EV, Kagadei VA, Kazimirov AI, et al. High threshold voltage p-gate GaN transistors. In: 2015 International Siberian Conference on Control and Communications (SIBCON). Omsk, 2015. 1–4

13 Han Y, Xue S, Guo W, et al. Highly selective dry etching of GaN over AlGaN using inductively coupled $Cl_2/N_2/O_2$ plasmas. Jpn J Appl Phys, 2003, 42: L1139–L1141

14 Wang L, Li L, Xie T, et al. Threshold voltage tuning in AlGaN/GaN

HFETs with p-type Cu_2O gate synthesized by magnetron reactive sputtering. Appl Surf Sci, 2018, 437: 98–102

15 Suzuki A, Choe S, Yamada Y, et al. NiO gate GaN-based enhancement-mode hetrojunction field-effect transistor with extremely low on-resistance using metal organic chemical vapor deposition regrown Ge-doped layer. Jpn J Appl Phys, 2016, 55: 121001

16 Zhang T, Wang L, Li X, et al. Positive threshold voltage shift in AlGaN/GaN HEMTs with p-type NiO gate synthesized by magnetron reactive sputtering. Appl Surf Sci, 2018, 462: 799–803

17 Huang SJ, Chou CW, Su YK, et al. Achievement of normally-off AlGaN/GaN high-electron mobility transistor with p-NiO_x capping layer by sputtering and post-annealing. Appl Surf Sci, 2017, 401: 373–377

18 Kaneko N, Machida O, Yanagihara M, et al. Normally-off AlGaN/GaN HFETs using NiO_x gate with recess. In: 2009 21st International Symposium on Power Semiconductor Devices & IC's. Barcelona, 2019. 25–28

19 Li G, Li X, Zhao J, et al. Design principle for a p-type oxide gate layer on AlGaN/GaN toward normally-off HEMTs: Li-doped NiO as a model. J Mater Chem C, 2020, 8: 1125–1134

20 Quackenbush NF, Allen JP, Scanlon DO, et al. Origin of the bipolar doping behavior of SnO from X-ray spectroscopy and density functional theory. Chem Mater, 2013, 25: 3114–3123

21 Ogo Y, Hiramatsu H, Nomura K, et al. p-Channel thin-film transistor using p-type oxide semiconductor, SnO. Appl Phys Lett, 2008, 93: 032113

22 Liang LY, Liu ZM, Cao HT, et al. Microstructural, optical, and electrical properties of SnO thin films prepared on quartz via a two-step method. ACS Appl Mater Interfaces, 2010, 2: 1060–1065

23 Lee HN, Kim HJ, Kim CK. p-Channel tin monoxide thin film transistor fabricated by vacuum thermal evaporation. Jpn J Appl Phys, 2010, 49: 020202

24 Fortunato E, Barros R, Barquinha P, et al. Transparent p-type SnO_x thin film transistors produced by reactive RF magnetron sputtering followed by low temperature annealing. Appl Phys Lett, 2010, 97: 052105

25 Li X, Liang L, Cao H, et al. Determination of some basic physical parameters of SnO based on SnO/Si pn heterojunctions. Appl Phys Lett, 2015, 106: 132102

26 Li Y, Yang J, Wang Y, et al. Complementary integrated circuits based on p-type SnO and n-type IGZO thin-film transistors. IEEE Electron Device Lett, 2018, 39: 208–211

27 Uemoto Y, Hikita M, Ueno H, et al. Gate injection transistor (GIT)—A normally-off AlGaN/GaN power transistor using conductivity modulation. IEEE Trans Electron Devices, 2007, 54: 3393–3399

28 Liu S, Song X, Zhang J, et al. Comprehensive design of device parameters for GaN vertical trench MOSFETs. IEEE Access, 2020, 8: 57126–57135

29 Li L, Wang W, He L, et al. Synthesis and characterization of p-type NiO films suitable for normally-off AlGaN/GaN HFETs application. Mater Sci Semicond Process, 2017, 67: 141–146

30 Chen CC, Chang WH, Yoshimura K, et al. An efficient triple-junction polymer solar cell having a power conversion efficiency exceeding 11%. Adv Mater, 2014, 26: 5670–5677

31 Erre R, Legay MH, Fripiat JJ. Reaction of molecular hydrogen with the 100 face of MoO_3. Surf Sci, 1983, 127: 69–82

32 Zhang TN, Wang SX, Wei W, et al. Atomic-Layer-Deposited ultrathin films of vanadium pentoxide crystalline nanoflakes with controllable thickness and optical band-gap. J Infrared Millim W, 2019, 38: 1–7

33 Iwata N, Kondo T. High-selectivity dry etching for p-type GaN gate formation of normally-off operation high-electron-mobility transistor. Jpn J Appl Phys, 2021, 60: SAAD01

34 Zhao SL, Wang ZZ, Chen DZ, et al. 1.8-kV circular AlGaN/GaN/AlGaN double-heterostructure high electron mobility transistor. Chin Phys B, 2019, 28: 027301

35 Xu N, Hao R, Chen F, et al. Gate leakage mechanisms in normally off p-GaN/AlGaN/GaN high electron mobility transistors. Appl Phys Lett, 2018, 113: 152104

36 Du J, Xia C, Liu Y, et al. Electronic characteristics of p-type transparent SnO monolayer with high carrier mobility. Appl Surf Sci, 2017, 401: 114–119

37 Guzmán-Caballero DE, Quevedo-López MA, Ramírez-Bon R. Optical properties of p-type SnO_x thin films deposited by DC reactive sputtering. J Mater Sci-Mater Electron, 2019, 30: 1366–1373

38 Sivaramasubramaniam R, Muhamad MR, Radhakrishna S. Optical properties of annealed tin(II) oxide in different ambients. Phys Stat Sol A, 1993, 136: 215–222

39 Guo W, Fu L, Zhang Y, et al. Microstructure, optical, and electrical properties of p-type SnO thin films. Appl Phys Lett, 2010, 96: 042113

40 Ťapajna M, Kuzmík J. A comprehensive analytical model for threshold voltage calculation in GaN based metal-oxide-semiconductor high-electron-mobility transistors. Appl Phys Lett, 2012, 100: 113509

41 Irokawa Y, Nabatame T, Yuge K, et al. Investigation of Al_2O_3/GaN interface properties by sub-bandgap photo-assisted capacitance-voltage technique. AIP Adv, 2019, 9: 085319

42 Miczek M, Mizue C, Hashizume T, et al. Effects of interface states and temperature on the C-V behavior of metal/insulator/AlGaN/GaN heterostructure capacitors. J Appl Phys, 2008, 103: 104510

43 Qu Y, Yang J, Li Y, et al. Organic and inorganic passivation of p-type SnO thin-film transistors with different active layer thicknesses. Semicond Sci Technol, 2018, 33: 075001

44 Fortunato E, Barquinha P, Martins R. Oxide semiconductor thin-film transistors: A review of recent advances. Adv Mater, 2012, 24: 2945–2986

45 Li Y, Yang J, Qu Y, et al. Ambipolar SnO_x thin-film transistors achieved at high sputtering power. Appl Phys Lett, 2018, 112: 182102

46 Bakeroot B, Stockman A, Posthuma N, et al. Analytical model for the threshold voltage of p-(Al)GaN high-electron-mobility transistors. IEEE Trans Electron Devices, 2018, 65: 79–86

Author contributions   Chen D conceived the idea, designed and guided the simulation calculation and experiment. Yuan P completed most of the calculations and experiments, and wrote the manuscript under Chen D's guidance. Yan S deposited the p-SnO film under the guidance of Xin Q. Chen D and Zhao S revised the manuscript. Zhang Y and Zhang C contributed to the epitaxial growth of AlGaN/GaN structure and device fabrication. Liu S, Song X, Zhang J, Zhang W, Zhu W, Xi H, and Zhou H helped with the model calibration, device measurement, film characterization, and data analysis. Zhang J and Hao Y supervised the group. All authors read and approved the manuscript.

Conflict of interest   The authors declare that they have no conflict of interest.

Supplementary information   Experimental details and supporting data are available in the online version of this paper.

Peng Yuan received his bachelor degree in microelectronics science and engineering from Xidian University in 2019. Now, he is a graduate student in Prof. Chen's group. His current research interests are concentrating on GaN power electronic devices.

Dazheng Chen obtained his BE and PhD degrees from Xidian University in 2010 and 2015, respectively, and entered the Post-doctoral Research Station of Physics in 2016. In 2018, he joined the School of Microelectronics, Xidian University, and is now an associate professor at the School of Microelectronics. His research interests focus on wide-bandgap semiconductor power devices and photo-electric devices.

Jincheng Zhang (Member, IEEE) received the MS and PhD degrees from Xidian University, Xi'an, China, in 2001 and 2004, respectively. He is currently a professor at Xidian University, Xi'an. His current interests include wide-bandgap semiconductor GaN and diamond materials and devices.

基于p-SnO帽层栅的高阈值增强型AlGaN/GaN HEMTs

陈大正[1†*]，袁鹏[1†]，赵胜雷[1]，刘爽[1]，辛倩[2]，宋秀峰[1]，颜世琪[2]，张雅超[1]，习鹤[1]，朱卫东[1]，张苇杭[1]，张家祺[1]，周弘[1]，张春福[1]，张进成[1*]，郝跃[1]

摘要 目前，p-GaN帽层技术是实现增强型GaN基HEMT的主流商用技术，但Mg掺杂难激活以及刻蚀损伤等因素限制了器件性能的进一步提升，因此高性能、低成本的增强型帽层技术具有重要的研究意义. 本文采用p型氧化亚锡(p-SnO)代替p-GaN作为栅帽层引入AlGaN/GaN HEMT，并通过Silvaco器件仿真和实验验证两方面系统研究了器件的电学性能. 仿真结果显示，通过简单改变p-SnO的厚度(50–200 nm)或掺杂浓度(3×10^{17}–3×10^{18} cm^{-3})，可以实现器件阈值电压在0–10 V范围内连续可调，同时器件的漏极电流密度超过120 mA mm^{-1}，栅击穿和器件击穿电压分别达到7.5和2470 V. 在此基础上，我们实验制备了基于磁控溅射p-SnO帽层的AlGaN/GaN HEMT，未经优化的器件测得了1 V的阈值电压、4.2 V的栅击穿电压和420 V的器件击穿电压，证实了p-SnO薄膜作为增强型GaN基HEMT栅帽层的应用潜力，为进一步提升增强型AlGaN/GaN HEMT性能，同时降低成本奠定了基础.